Chemical Physics 536 (2020) 110810

Contents lists available at ScienceDirect

Chemical Physics

journal homepage: www.elsevier.com/locate/chemphys

Charge reversal in the collapse of polyelectrolyte star brushes under an electric field

Tianbao Wang, Shaoyun Wang, Chaohui Tong*

Department of Physics, School of Physical Science and Technology, Ningbo University, Ningbo, Zhejiang 315211, China

A B S T R A C T

We have performed Langevin dynamics simulations of the collapse of charged star brushes under an external electric field. It was found that the emergence of charge reversal of collapsed charged monomers on the grafting electrode is governed by the total net charge on a single grafted ordinary polyelectrolyte or polyampholyte chain. The mean value of the total net charge on a grafted star chain required to induce charge reversal on the grafting electrode decreases with increasing Bjerrum length. However, at very high Bjerrum length, the grafted star chains with ionizable functional groups are effectively neutral. Thus, the phenomenon of charge reversal becomes irrelevant at very high Bjerrum length. Simulation results revealed that the thickness of the adsorption layer is nearly independent of the average charge fraction, arm length and number of arms of grafted star chains as well as Bjerrum length. In the regime of charge reversal, simulation results showed that the degree of charge overcompensation increases with increasing charge fraction, but is nearly irrespective of the arm length and number of arms of grafted star chains. The degree of charge overcompensation was found to be a non-monotonic function of Bjerrum length and it reaches a maximum at an intermediate value of Bjerrum length. The effects of the characteristic parameters of grafted star chains and the applied electric field on the internal stratification of polyelectrolyte star brushes were also examined.

1. Introduction

The adsorption of polyelectrolytes (PE) on oppositely charged surfaces is interesting and fascinating from a physics point of view and is also of great technological importance due to numerous applications in industries such as paint making, water treatment, food processing, etc. [1–8]. PE adsorption is not limited to the realm of traditional charged polymers. The adsorption and complexation of bio-macromolecules such as DNA onto the surfaces of oppositely charged proteins and membranes, and more specifically, the complexation of histone-DNA in nucleosomal core particles are examples of PE adsorption in the biological context. Therefore, PE adsorption has generated intense interest in the theoretical and computational polymer physics community [2–19]. Previous studies examined the adsorption-depletion transition, the effects of added salt ions and solution pH, image charge effect of the substrate and the influences of the linear charge density and rigidity of polyelectrolyte chains as well as the curvature effect of the adsorbing surface in the weak adsorption regime [9–17]. Moreover, the various polyelectrolyte adsorption patterns on cylindrical and spherical objects and their stabilities in the strong adsorption regime have also been investigated [18,19].

A particular fascinating phenomenon of PE adsorption is charge reversal on oppositely charged objects. That is, the adsorbed charged monomers charge overcompensate the opposite surface charges. Charge reversal is the underlying mechanism of layer-by-layer deposition to prepare supported multilayer polymer thin films by sequential adsorptions of cationic and anionic polyelectrolytes [20]. It is well recognized that charge correlation is the main driving force for charge reversal. However, short-range specific interactions such as hydrophobic/hydrophilic interactions and hydrogen bonding can also play important roles in charge reversal [21,22].

A scenario of PE adsorption which has been overlooked is the adsorption of PE brushes onto the oppositely charged grafting substrate. PE brushes made of polyelectrolyte chains densely end-tethered to solid substrates can modify and improve the physiochemical properties of solid substrates, and thus can be used to fabricate smart surface layers with a wide range of technological applications [23–33]. For example, the response of PE brushes to external electric fields or voltage has been utilized in sensing and actuation [25]. Under a collapsing electric field applied normal to the grafting substrate, the polyelectrolyte chains are adsorbed onto the oppositely charged grafting electrode. Self-consistent field theory calculations of PE brushes collapsing in external electric fields showed that an exact charge neutralization of the grafting electrode by adsorbed charged monomers is established [34,35]. Molecular dynamics simulations revealed that under the condition of Bjerrum length much smaller than the monomer diameter, the adsorbed charged monomers exactly charge compensate the opposite surface charges on the grafting electrode [36]. However, our recent simulation study of 3-

* Corresponding author.
E-mail address: tongchaohui@nbu.edu.cn (C. Tong).

https://doi.org/10.1016/j.chemphys.2020.110810
Received 23 December 2019; Received in revised form 25 March 2020; Accepted 13 April 2020
Available online 16 April 2020
0301-0104/

arm polyelectrolyte star brushes under external electric fields unequivocally demonstrated that charge overcompensation at the grafting electrode surface can emerge for PE chains with relatively high charge fraction [37].

In this work, by performing extensive Langevin dynamics simulations, we investigated charge reversal of the grafting electrode by collapsed charged star brushes. Large parameter spaces in terms of the average charge fraction, arm length and number of arms of grafted star chains as well as Bjerrum length were explored to decipher the criterion governing the emergence of charge reversal at the grafting electrode. The effects of these parameters on the degree of charge overcompensation were examined. Furthermore, the influence of these parameters on the stratification within the brush layer was investigated. To further elucidate the underlying physics regarding the emergence of charge reversal of polyelectrolyte brushes at the grafting electrode, polyelectrolyte brushes made of polyampholyte chains consisting of positive, negative and neutral monomers were investigated. Compared with our previous study of 3-arm polyelectrolyte brushes under external electric field in which the condition for the emergence of charge reversal of the grafting electrode was only qualitatively discussed, the criterion governing charge reversal was quantitatively investigated by exploring large parameter space in this work. The effect of Bjerrum length on charge reversal was investigated in the current study. Moreover, the effects of charge pattern and charge distribution on polymer chains on the adsorption of polyelectrolyte brushes and charge reversal at the grafting electrode were quantitatively studied. The rest of the paper is organized as follows. The model and simulation detail are described in Section 2. Simulation results and discussion are elaborated in Section 3. In Section 4, the main results of this work are summarized and conclusions are drawn.

2. Model and method

In this study, the polyelectrolyte star brushes consist of $M = 8 \times 8$ flexible f- arm stars uniformly grafted on a planar electrode with dimensions $L_x \times L_y$ at $z = 0$. A second planar electrode at $z = L_z$ establishes a planar capacitor with grafted star chains and released counterions immersed in an aqueous solution sandwiched between the two oppositely charged electrodes. In the x- and y- directions the periodic boundary conditions were applied. The grafting density of the brush is given by $\sigma_g = M/(L_x L_y)$. The standard coarse-grained bead-spring model was employed in the simulations. Neutral and negatively charged monomers as well as positively charged monovalent counterions were modeled as spherical Lennard-Jones (LJ) beads (σ, ε) with equal diameter σ and mass m. The finitely extensible nonlinear elastic (FENE) bond potential was adopted to maintain the connectivity of two neighboring monomers on the same arm. The end monomer of one of the f arms of a star chain (the stem) was uniformly anchored on the square lattice at $z = 0$. The f arms of a star chain are connected to a central monomer which is also called the branching point in the main text. The number of arms of grafted star chains f was varied from 2 to 6. Please note that $f = 2$ corresponds to a linear chain. Each arm of a f-arm star chain is made up of N monomer units and N was selected from $N \in \{30, 45, 60, 75, 90\}$ in the simulations. The charge fraction of f- arm stars α was chose from $\alpha \in \{1/3, 1/5, 1/7, 1/9, 1/11\}$ in the simulations. The charged monomers are uniformly distributed along the arms of star chains separated by equal number of neutral monomers. For example, if $\alpha = 1/3$, then two neighboring charged monomers each carrying a negative charge (in units of elementary electronic charge) are separated by two neutral monomers in each arm of a star macromolecule. The schematic illustration of the brush system is shown in Fig. 1.The methodological detail of the simulations can be found elsewhere [37].

The time evolution of the particles in the brush system follows the standard Langevin dynamics which is an implicit solvent model. The temperature of the system was set to $k_B T = 1.2\varepsilon$ with ε standing for the amplitude of LJ potential [37], and the friction coefficient $\zeta = 1.0 m\tau^{-1}$ with $\tau = \sigma(m/\varepsilon)^{1/2}$ denoting the time unit [37]. In this study, we set the size of all the particles as $\sigma = 0.237$ nm, which is approximately equal to the bond length of Polystyrene Sulfonate (PSS) [37]. The effect of the strength of electrostatic interaction on charge reversal of charged monomers collapsing onto oppositely charged grafting electrode was investigated. Bjerrum length was varied from 2σ to 18σ in the simulations. The larger Bjerrum length, the stronger the electrostatic interaction between charged particles will be. For simplicity, the effect of the solvent quality on charge reversal was not studied. An external electric field $\overrightarrow{E}$ was applied along the positive z direction which exerts a force $eq\overrightarrow{E}$ on a charged particle (e denotes an elementary charge and $q = +1$ and $q = -1$ for monovalent counterions and charged monomers, respectively), thus driving the collapse of the charged star brushes onto the grafting electrode. The LD unit of the external electric field is $\varepsilon/(e\sigma) = k_B T/(1.2e\sigma) \cong 9.0 \times 10^7$V/m. In this work, the electric field strength was fixed to be $|\overrightarrow{E}| = 1.0$ corresponding to 9.0×10^7V/m. Such a field strength is consistent with experimental observations [38]. In this work, the dimensionless grafting density $\sigma *_g \equiv \sigma_g \sigma^2$ was fixed at 0.005, which lies in the low grafting density regime where the response of PE brushes to electric fields is strong due to the low degree of electrostatic screening from charged species.

3. Results and discussions

3.1. Stratification within the brush layer

The emergence of internal stratification with some grafted branched polymer chains retracting towards the grafting substrate to fill the void near the grafting substrate is a unique feature of branched polymer brushes compared with linear polymer brushes. The grafted star chains can be classified as all-up, all-down and intermediate chains. The population weights of grafted chains in these three different conformations were calculated as follows. The average vertical coordinate of the branching points (the branching point refers to the central monomer connected by all the arms of a star chain) of all grafted star chains was used to demarcate the boundary between the all-up and all-down conformations. A grafted star chain with all of its monomers below the average height of the branching points was regarded to be in the all-down conformation. Conversely, a grafted star chain with all of the monomers in all the free branches above that average height is in the all-up conformation. The rest of the grafted chains are in the intermediate state.

The effects of the arm length and charge fraction of grafted chains as well as the collapsing electric field on the probability distribution of the branching points are shown in Fig. 2(a) and (b). In the absence of external electric field, due to the relatively low grafting density, the probability distribution $\phi_b(z)$ of the branching points exhibits a unimodal distribution at short arm length and low charge fraction. With increasing arm length N and charge fraction α, $\phi_b(z)$ exhibits bimodal/multimodal distribution, signaling the emergence of internal stratification inside the brush layer. Increasing the number of arms in a star chain has a similar effect on the probability distribution of the branching points. Under a collapsing external electric field, a new peak in the probability distribution of the branching points emerges in the immediate vicinity of the grafting electrode, indicating that some grafted star chains are attracted towards the grafting electrode to charge compensate the opposite surface charges. The weight fraction of the new peak near the grafting electrode decreases with increasing arm length and charge fraction. In Fig. 3(a) and (b), the effects of the arm length and charge fraction of grafted chains as well as the collapsing electric field on the weight fractions of the different chain conformations are displayed. Clearly, compared with the case of no applied electric field, the population weight of the grafted chains in the all-down conformation grows at the expense of the chains in the immediate state under a collapsing electric field, and the population weight of the

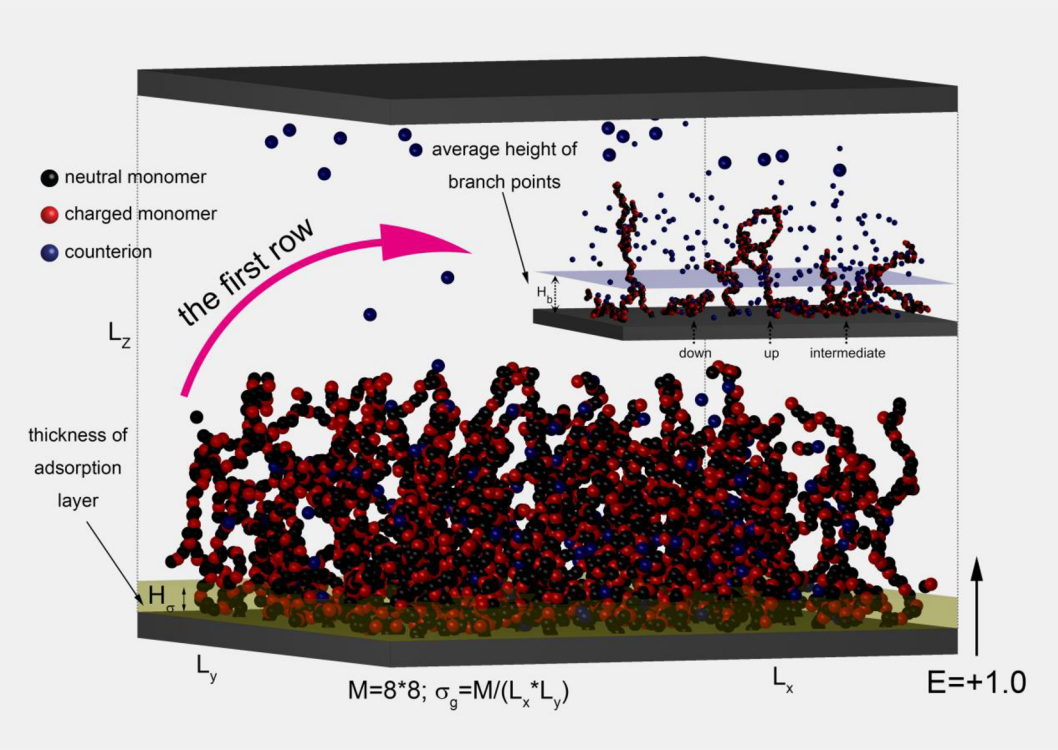

Fig. 1. Schematic illustration of the brush system composed of 8 × 8 star chains with negatively charged monomer (red particles) evenly distributed along the arms uniformly grafted on a square substrate located at z = 0 under a collapsing electric field. The different chain conformations of up, down and intermediate are defined in the first paragraph in subsection 1 of Section 3. The adsorption layer and its thickness are defined in the first paragraph in subsection 4 of Section 3.

chains in the all-up conformation is not affected much by the applied electric field.

4. Condition for the emergence of charge reversal on the charged grafting electrode

In previous MD simulation studies, we have demonstrated that for PE brushes collapsing in an external electric field, charge overcompensation from collapsed charged monomers on oppositely charged grafting electrode takes place if the average charge fraction and chain length of grafted chains are high enough [37]. A key indicator of the emergence of charge reversal on the charged grafting electrode is that some counterions with the same charge sign as the surface charges of the electrode accumulate in the immediate vicinity of the electrode. Nevertheless, if the contributions of both the collapsed charged monomers and counterions are taken into account, approximate charge neutrality near the grafting electrode is established. In this work, in order to find the condition for the emergence of charge reversal on the grafting electrode, the probability density distributions of counterions under a collapsing electric field and in the absence of electric fields were compared for PE star brushes with different average charge fraction, arm length and number of arms. If there is a peak in the probability distribution of counterions in the immediate vicinity of the grafting electrode under a collapsing electric field, which lies above the probability distribution of counterions in the absence of electric fields, we conclude that charge reversal on the grafting electrode takes place. It can be clearly seen from Fig. 4(a) that, for PE star brushes with $f = 3$, $N = 45$, $\alpha = 1/3$ collapsing in an electric field, charge reversal on the

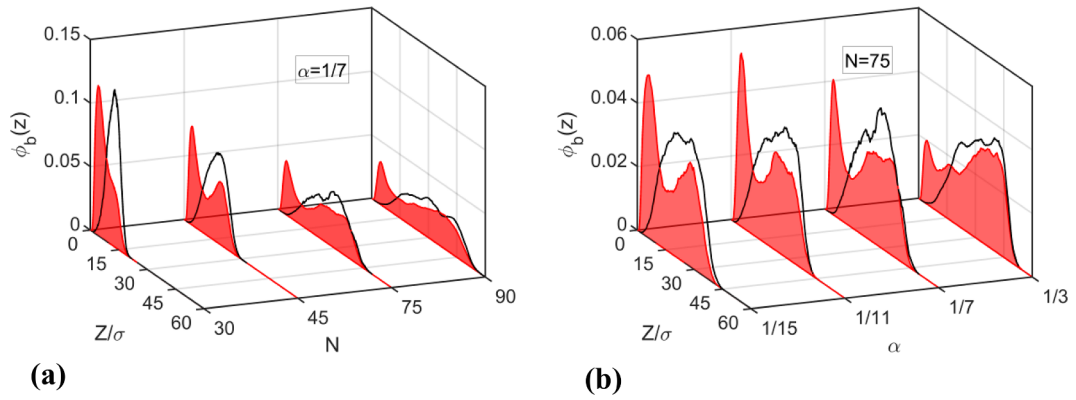

Fig. 2. (a) Normalized probability distributions of the branching points of 3-arm star brushes with charge fraction of 1/7 at a grafting density of $\sigma_g^* = 0.005$ at different arm lengths in the absence of electric fields (black solid curves) and under an electric field $E = 1.0$(red filled curves). (b) Normalized probability distributions of the branching points of 3-arm star brushes with arm length of 75 at a grafting density of $\sigma_g^* = 0.005$ at different charge fractions in the absence of electric fields (black solid curves) and under an electric field $E = 1.0$ (red filled curves).

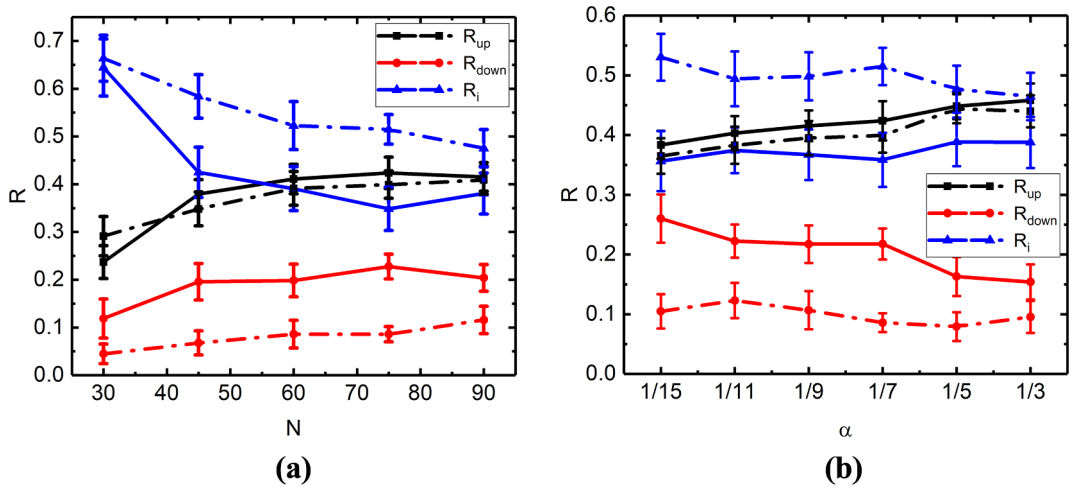

Fig. 3. (a) Fractions of grafted chains in the all-up R_{up}, all-down R_{down} and intermediate state R_I as a function of the arm length of 3-arm star brushes with charge fraction of 1/7 at a grafting density of $\sigma_g^* = 0.005$ in the absence of electric fields (dash-dotted curves) and under an electric field $E = 1.0$(solid curves). (b) Fractions of grafted chains in the all-up R_{up}, all-down R_{down} and intermediate state R_I as a function of the charge fraction of 3-arm star brushes with an arm length $N = 75$ at a grafting density of $\sigma_g^* = 0.005$ in the absence of electric fields (dash-dotted curves) and under an electric field $E = 1.0$ (solid curves).

grafting electrode takes place. However, for PE star brushes with much smaller charge fraction than the aforementioned brushes, no charge reversal emerges on the grafting electrode (see (b) of Fig. 4).

We conducted extensive simulations and constructed phase diagrams in terms of different pairs of average charge fraction, arm length and number of arms of grafted star chains, which demarcate the charge reversal and non-reversal regimes of charged monomers collapsing onto oppositely charged grafting electrode. As shown in Fig. 5, the charge reversal regimes are all located in the upper right corners of the phase diagrams. Thus, charge reversal on the grafting electrode by collapsed oppositely charged monomers entails large values of average charge fraction, arm length and/or number of arms of the grafted star chains. It turns out that the emergence of charge reversal on the grafting electrode depends critically on the total number of charges carried by a grafted polymer chain. At Bjerrum length of 3σ, based on the phase diagrams shown in Fig. 5, it was found that the mean value of the total number of charges carried by a grafted chain for the emergence of charge reversal is about $N_q = f{\cdot}N{\cdot}\alpha \approx 30$. The minimum value of the total number of monomer charges on a grafted chain needed to induce charge reversal is about 26. For star brushes with $f = 6$, $N = 45$, $\alpha = 1/11$ corresponding to $N_q = f{\cdot}N{\cdot}\alpha \approx 25$, no charge reversal takes place. However, for star brushes with $f = 3$, $N = 60$, $\alpha = 1/7$ corresponding to $N_q = f{\cdot}N{\cdot}\alpha \approx 26$, charge reversal takes place.

5. Effect of Bjerrum length on charge reversal on the charged grafting electrode

The electrostatic interaction between charged monomers and the released counterions as well as oppositely charged surface charges on the grafting electrode exerts great influence on the adsorption of charged monomers onto the electrode. Bjerrum length is a quantitative measure of the strength of electrostatic energy relative to the thermal energy. Phase diagrams in terms of different pairs of average charge fraction, arm length and number of arms of grafted star chains, which demarcate the charge reversal and non-reversal regimes of charged monomers collapsing onto oppositely charged grafting electrode, were constructed at different Bjerrum lengths and are shown in Fig. 6 (typical conformations of polyelectrolyte star brushes under a collapsing electric field in charge reversal and non-reversal subdomains are shown in Fig. S1 in the Supporting Information). The regimes of charge reversal at the smallest Bjerrum length of $l_B = 2\sigma$ investigated in this work occupy the top right corners of the phase diagrams. As Bjerrum length increases, the regime of charge reversal expands towards the lower left corner of the phase diagram corresponding to smaller values of average charge fraction, arm length and number of arms. Therefore, the mean value of the total number of charges carried by a grafted chain required for the emergence of charge reversal decreases with increasing Bjerrum

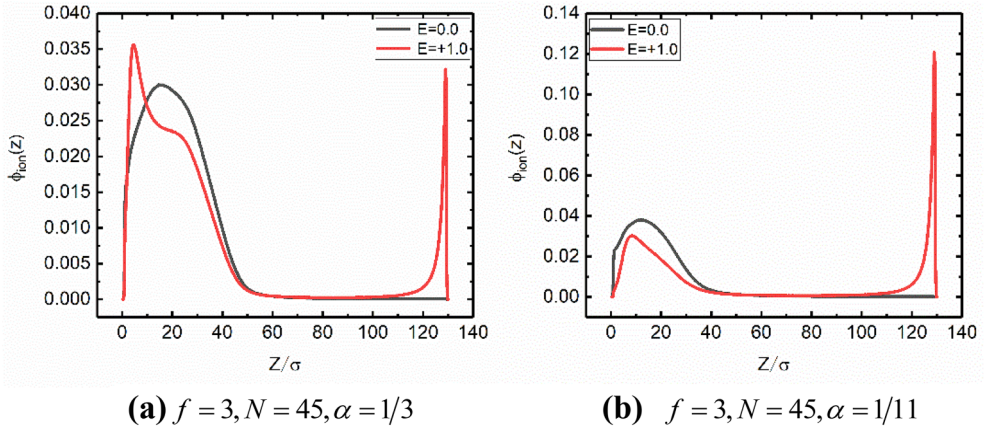

Fig. 4. Normalized probability density distributions of counterions of star brushes with different characteristic parameters at different electric field strengths.

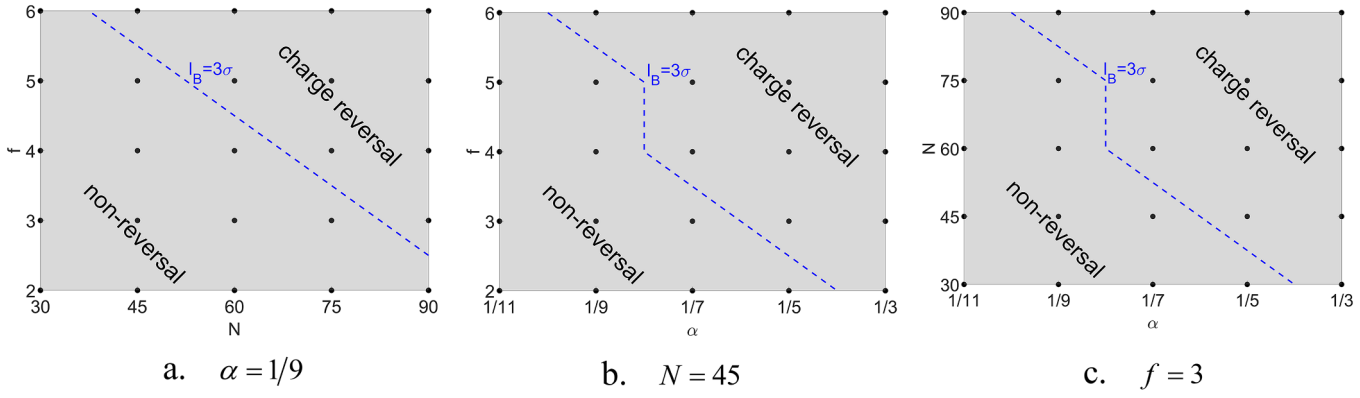

Fig. 5. Phase diagrams in terms of charge fraction, arm length and number of arms of grafted star chains demarcating charge reversal region and non-reversal regions. Note that the region in the upper right of the boundary line (broken blue line) corresponding to larger total number of charged monomers in a single grafted chain denotes the charge reversal subdomain. In these phase diagrams, $l_B = 3\sigma$.

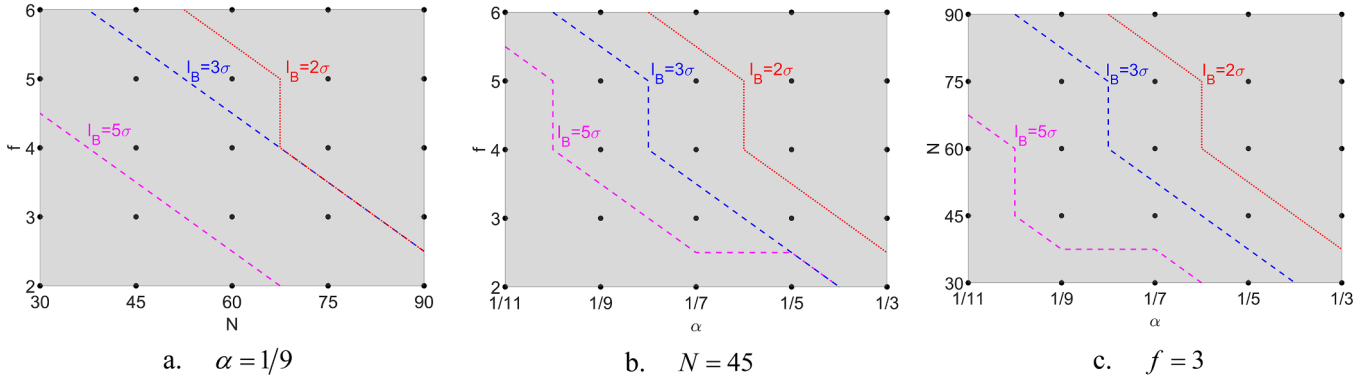

Fig. 6. Phase diagrams demarcating charge reversal region and non-reversal region at different charge fractions, arm lengths and number of arms of grafted star chains for different Bjerrum lengths. For each boundary line at a particular Bjerrum length, the phase region in the upper right of it corresponds to the charge reversal subdomain, and the phase region in the lower left of it corresponds to the non-reversal subdomain.

length as shown in Fig. 7. This is due to the fact that the larger Bjerrum length is, the longer range of the electrostatic interaction between the surface charges on the grafting electrode and the oppositely charged monomers will be.

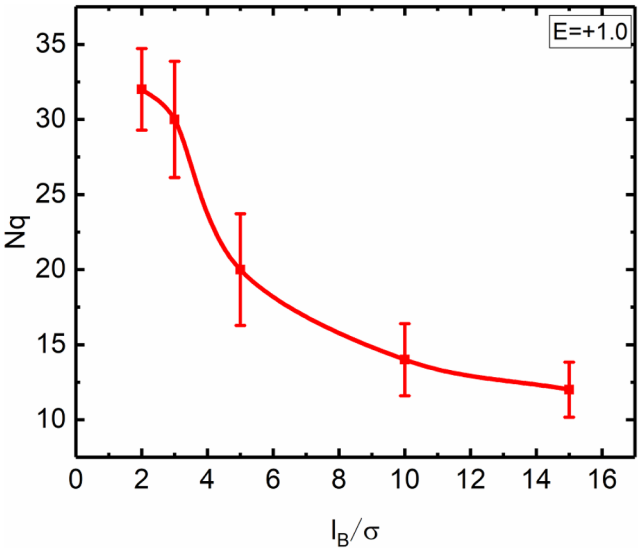

Fig. 7. The mean value of total number of charged monomers in one grafted star chain needed to induce charge reversal on the grafting electrode as a function of Bjerrum length.

6. Degree of charge overcompensation on the charged grafting electrode

In order to quantify the degree of charge overcompensation, the adsorption layer near the grafting electrode was identified first. The probability density distribution of charged monomers was employed to demarcate the adsorption layer near the grafting electrode. As shown in Fig. 8, in the immediate vicinity of the grafting electrode, there is a sharp peak in the probability distribution of charged monomers which is on top of the corresponding distribution in the absence of electric fields. The vertical position of the intersecting point of these two normalized probability distributions can be found. The region from $z = 0$ to the z coordinate of the intersecting point was defined as the adsorption layer. It was found that the thickness of the adsorption layer is about 9σ irrespectively of the average charge fraction, arm length and number of arms of grafted star chains. Moreover, the vertical position of the intersecting point of normalized probability distributions of all monomers was also found to be around 9σ and is irrespectively of the average charge fraction, arm length and number of arms of grafted star chains. It is interesting to compare the dependences of the thickness of adsorption layer on the characteristic parameters of PE chains in the case of grafted PE chains (PE brushes) with those in the case of free PE chains. Theoretical study and SCFT calculation revealed that the thickness of the adsorption layer in the case of free PE chains is independent of the chain length and scales with the charge fraction as a power law with an exponent of $-1/3$ [17,39].

With the definition of the adsorption layer, the degree of charge overcompensation Ξ can be calculated from the following expression:

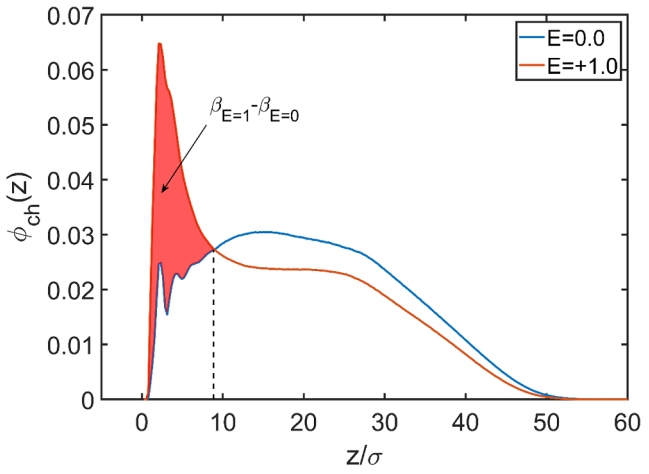

Fig. 8. A schematic diagram demarcating the adsorption layer near the grafting electrode by using the normalized probability distributions of charged monomers at electric field strengths of $E = 1$ and $E = 0$.

$$\Xi = \frac{eN_q(\beta_{E=1} - \beta_{E=0})}{s\sigma_e} - 1 = \frac{4.8\pi(l_B/\sigma)\sigma *_g N_q(\beta_{E=1} - \beta_{E=0})}{E} - 1 \quad (1)$$

with σ_e denoting the surface charge density on the two oppositely charged electrodes ($\sigma_e = \varepsilon_0\varepsilon_r |\overrightarrow{E}|$ in SI unit with ε_0, ε_r denoting the vacuum permittivity and the dielectric constant of water, respectively), and s standing for the average surface area occupied by one grafted chain ($s = 1/\sigma_g = \sigma^2/\sigma *_g$). In the above equation, and $\beta_{E=0}$ denote the weight fractions of charged monomers inside the adsorption layer under electric field strengths of $E = 1$ and $E = 0$, respectively (see Fig. 7). Note that in Eq. (1), the dimensionless electric field strength E is in LD unit of $\varepsilon/(e\sigma) = k_BT/(1.2e\sigma) \cong 9.0 \times 10^7$V/m. Therefore, in Eq. (1), $\sigma_e = \varepsilon_0\varepsilon_r |\overrightarrow{E}| = \varepsilon_0\varepsilon_r Ek_BT/(1.2e\sigma)$. Using the definition of Bjerrum length $l_B = e^2/(4\pi\varepsilon_0\varepsilon_r k_BT)$, the second equality in Eq. (1) is afforded. If $\Xi > 0$, charge overcompensation takes place near the grafting electrode.

It can be clearly seen from Fig. 9(a) that, the degree of charge overcompensation increases with increasing charge fraction of the grafted star chains. However, the degree of charge overcompensation has a very weak dependence on the number of arms of grafted star chains. Furthermore, Fig. 9(b) clearly shows that the arm length of grafted star chains has a very weak effect on the degree of charge overcompensation. The very weak dependence of the degree of charge overcompensation on the arm length and number of arms of grafted star chains is due to the nearly independence of the thickness of the adsorption layer on these two characteristics of grafted star chains. The total numbers of monomers inside the adsorption layer are about the same at different charge fractions, arm lengths and numbers of arms of grafted star chains. Thus the degree of charge overcompensation increases with increasing charge fraction. For a comparison, in the case of the adsorption of free PE chains in a solution onto an oppositely charged surface, SCFT calculations showed that the degree of charge overcompensation increases with both the charge fraction and chain length [17,39].

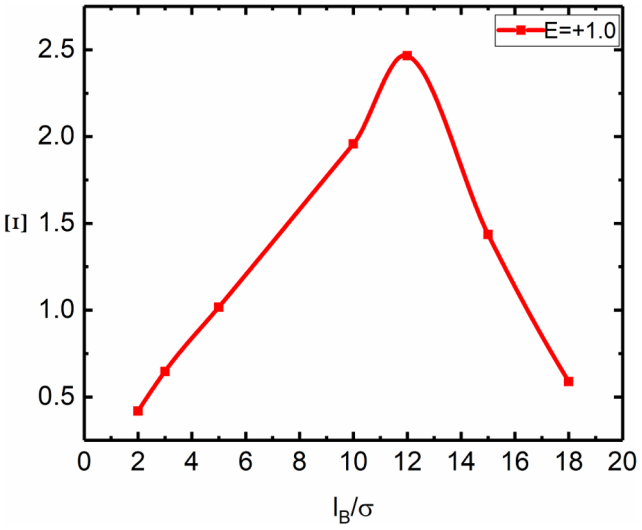

Fig. 10. Degree of charge overcompensation as a function of Bjerrum length. All the data points correspond to grafted star chains with $f = 3$, $N = 45$, $\alpha = 1/3$.

The effect of Bjerrum length on the degree of charge overcompensation was examined and the result is shown in Fig. 10. The degree of charge overcompensation initially increases with increasing Bjerrum length. After reaching a maximum, it decreases with increasing Bjerrum length. Such a non-monotonic change of the degree of charge overcompensation with Bjerrum length can be rationalized as follows. At very high Bjerrum length, the electrostatic interaction between charged monomers and their associated counterions are so strong that they tightly bind with each other, leading to neutral polymer chains

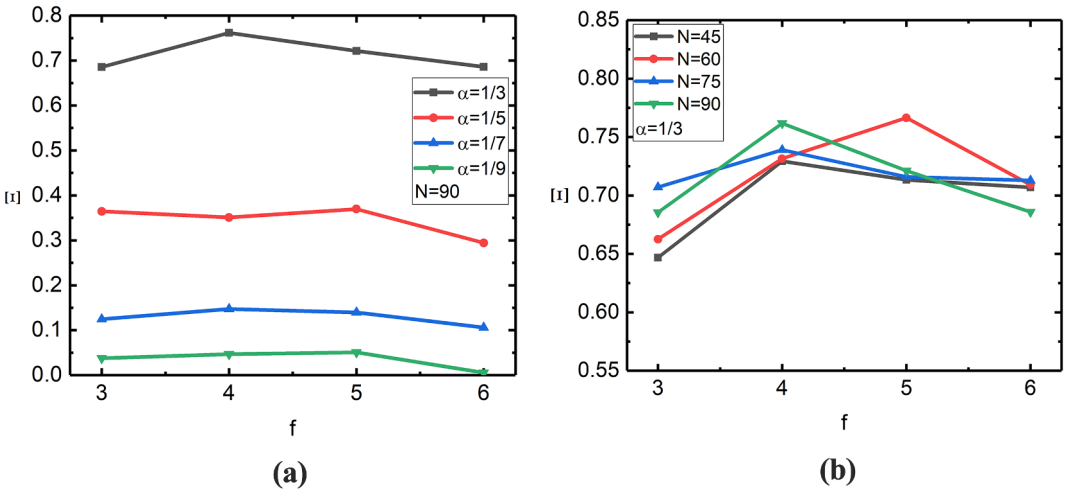

Fig. 9. (a) Degrees of charge overcompensation as a function of number of arms of the grafted chains at different charge fractions. Each arm has 90 monomers. (b) Degrees of charge overcompensation as a function of number of arms of the grafted chains at different arm lengths. The average charge fraction of grafted star chains is 1/3. In the figure, $l_B = 3\sigma$.

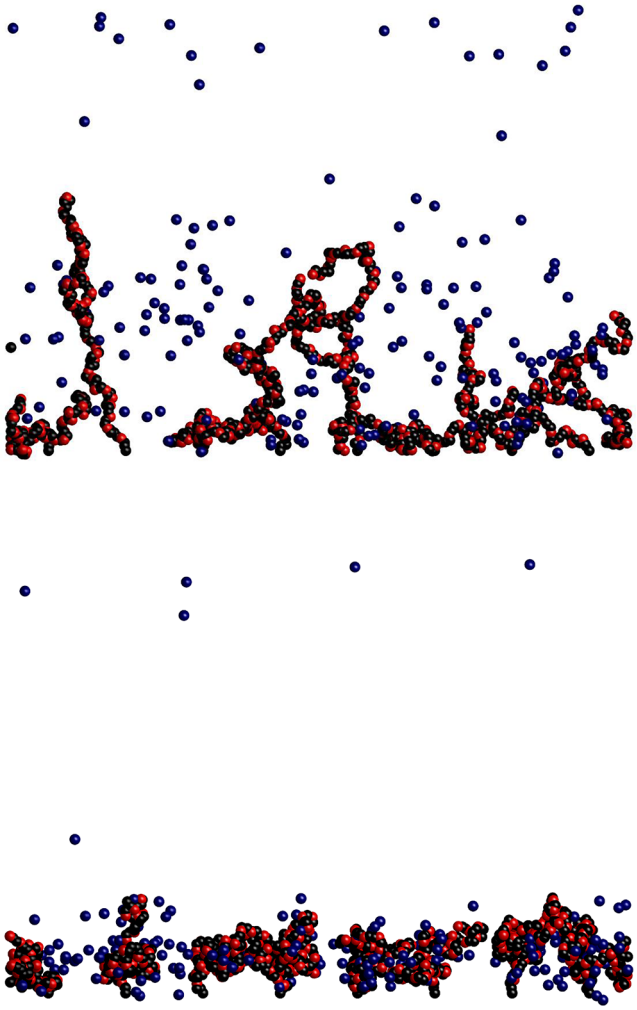

Fig. 11. Snapshots of a row of grafted 3-arm polyelectrolyte chains ($\alpha = 1/3$, $N = 45$) under a collapsing electric field ($E = 1.0$). The upper and lower figures correspond to Bjerrum length of 3σ, 15σ, respectively. In the figures, red, black and blue spheres represent charged monomers, neutral monomers and counterions, respectively. For better visualization, the counterions near the upper electrode have been repositioned downwards.

with completely no ionization of the ionizable functional groups on the polymer backbone. Thus, at very high Bjerrum length, the electrostatic interaction between grafted star chains and the charged electrode becomes irrelevant and the degree of charge overcompensation should be zero. It is a well recognized fact that charged polymers (polysalts) are insoluble in non-polar solvents which have very high values of Bjerrum length. In the low Bjerrum length limit in which the electrostatic interaction is very strongly screened by the solvent dipoles, the electrostatic interaction between charged species is so weak that the intermolecular van de Waals interaction becomes the dominant force. So the charged polymer chains behave like neutral ones. Thus the degree of charge overcompensation should be zero in the low Bjerrum length limit. Therefore, at some intermediate Bjerrum length, the degree of charge overcompensation reaches a maximum. It can be clearly seen from the snapshots of simulation shown in Fig. 11 that at larger Bjerrum length, the counterions are more tightly bound to charged monomers and the polymer chains are more compact compared with the case of smaller Bjerrum length (a video file illustrating the dynamics of polyelectrolyte star brushes under a collapsing electric field at different Bjerrum lengths can be found in the Supporting Information). Furthermore, it was found that the thickness of the adsorption layer has a very weak dependence on Bjerrum length. It should be pointed out that compared with changing the temperature, changing the dielectric constant of the solvent gives much greater lattitude to adjust Bjerrum length. For example, the dielectric constant of hydrocarbon solvent is one order of magnitude smaller than that of water.

7. Emergence of charge reversal on the grafting electrode by the collapsed polyampholyte star brushes

As a special type of charged polymer chains, polyampholyte (PA) chains have been used as model systems to study polypeptides composed of different amino-acid residues and disordered proteins. The adsorption of polyampholyte chains onto charged substrates have been extensively investigated experimentally and theoretically [40–46]. It would be very interesting to compare the adsorption behaviour regarding the emergence of charge reversal between ordinary polyelectrolyte brushes and polyampholyte brushes. In this work, both randomly charged and diblock polyampholyte star brushes were considered. In a polyampholyte chain with f arms each of which consists of N monomers, the charged monomers are uniformly positioned along the arms and these monomers are separated by equal number $(1/\alpha - 1)$ of neutral monomers. For randomly charged polyampholyte chains, the charged monomers are randomly chosen as either positively or negatively charged with a given probability p for a monomer to be negatively charged. Thus, the total net charge in units of electron for a randomly charged polyampholyte chain is $Nf\alpha(2p - 1)$. For diblock polyampholyte chains, either the stem (the grafted arm) or a free arm is positively charged while the rest arms are negatively charged. So for such a diblock polyampholyte star chain, the total net charge is $N\alpha(f - 2)$. Simulation results revealed that the emergence of charge reversal at the grafting electrode is not governed by the charge patterns (either randomly or block charged) and any particular values of N, f, α, p, but depends only on the total net charge of a grafted PA chain. Our preliminary simulation study as shown in Fig. 12 indicated that the total net charge of a PA chain required to induce charge reversal at the grafting electrode is about 24 at Bjerrum length of 3σ, which is very close to the lower bound of the total number of charges on a ordinary polyelectrolyte chain needed to induce charge reversal (see Fig. 7). Please note that the degree of charge overcompensation for

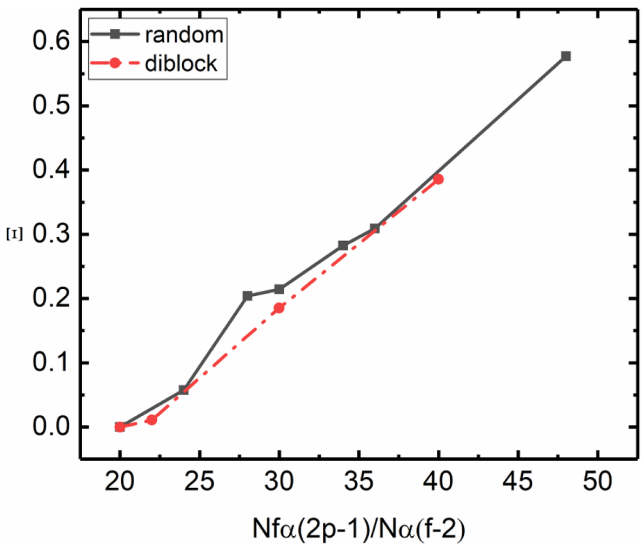

Fig. 12. Degree of charge overcompensation as a function of the total net charge of a grafted polyampholyte chain with different charge patterns (randomly charged and block charged) under a collapsing electric field ($E = 1.0$). The polyampholyte star brushes are made of 4-arm polyampholyte star chains ($N = 45$), and p was varied from 0.5 to 0.9 with $\alpha = 1/3$ for randomly charged PA chains. Note that the total net charge of a randomly and block charged PA chain is $Nf\alpha(2p - 1)$ and $N\alpha(f - 2)$, respectively. The Bjerrum length is 3σ.

polyampholyte chains is defined as the ratio of the total amount of net charges of PA chains inside the boundary layer to the amount of surface charges on the grafting electrode subtracted by 1. That is:

$$\Xi = \frac{eNf\alpha p(\beta^{-}_{E=1} - \beta^{-}_{E=0}) - eNf\alpha(1-p)(\beta^{+}_{E=1} - \beta^{+}_{E=0})}{s\sigma_e} - 1 \quad (2)$$

where $\beta^{\mp}$ denote the weight fractions of negatively and positively charged monomers inside the boundary layer respectively. Moreover, Fig. 12 clearly shows that the degree of charge overcompensation is nearly independent of the charge patterns in polyampholyte star chains.

It was found that under the condition of the total net charge on a PA star chain equal to the total charge on an ordinary polyelectrolyte star chain, the center of mass height of polyampholyte star brushes is smaller than that of polyelectrolyte star brushes with the same N, f and grafting density (see Fig. S2 in the Supporting Information). This is because the total amount of positive and negative charges on charged monomers and mobile ions per grafted PA chain is larger than that of only negatively charged monomers and positively charged counterions per grafted ordinary polyelectrolyte chain. Therefore, the electrostatic screening effect in the polyampholyte brush system is stronger than that in the ordinary polyelectrolyte brush system although the total net charge on a PA chain is equal to the total charge on a ordinary polyelectrolyte chain.

8. Conclusion

In this study we have performed Langevin dynamics simulations of the collapse of charged star brushes under an external electric field. We focused on the charge reversal of charged monomers adsorbed on the oppositely charged grafting electrode and the effects of the characteristic parameters of the grafted star chains and Bjerrum length on the degree of charge overcompensation on the grafting electrode by the adsorbed charged monomers. It was found that the emergence of charge reversal of collapsed charged monomers on the grafting electrode is governed by the total number of charged monomers in a single grafted chain, which is a product of the average charge fraction, arm length and number of arms of grafted star chains. The mean value of the total number of charges in a grafted star chain required to induce charge reversal on the grafting electrode decreases with increasing Bjerrum length. However, at very high Bjerrum length, the counterions are so tightly bound to charged monomers that charged polymer chains are effectively neutral. Thus, the phenomenon of charge reversal becomes irrelevant at very high Bjerrum length.

Simulation results revealed that the thickness of the adsorption layer is nearly independent of the average charge fraction, arm length and number of arms of grafted star chains as well as Bjerrum length. In the regime of charge reversal, simulation results showed that the degree of charge overcompensation increases with increasing charge fraction, but is nearly irrespective of the arm length and number of arms of grafted star chains. This is because inside the adsorption layer with almost constant thickness, the total numbers of collapsed monomers are about the same for star chains with different average charge fraction, arm length and number of arms. The degree of charge overcompensation was found to be a non-monotonic function of Bjerrum length and it reaches a maximum at an intermediate value of Bjerrum length. It can be anticipated that in the large and small limits of Bjerrum length, the degree of charge overcompensation will approach zero and the charged star chains behave like neutral polymers.

Simulation results regarding the collapse of polyampholyte star chains with different charge distributions (randomly or block charged) onto the grafting electrode under external electric fields showed that the emergence of charge reversal on the grafting electrode depends on the total net charge on a grafted polyampholyte chain. The total net charge was found to be close to the lower bound of the total charge on a ordinary polyelectrolyte chain required to induce charge reversal. Therefore, it is quite reasonable to conclude that for charged polymer brushes with quenched charged distribution, the emergence of charge reversal of charged monomers adsorbed on the oppositely charged grafting electrode is governed by the total net charge on a grafted chain, irrespective of the architectures (e.g., linear or star), characteristic parameters of the grafted chains (e.g., chain length), the types of charged chains (ordinary or polyampholyte) and the charge distributions on the grafted chains.

CRediT authorship contribution statement

Tianbao Wang: Investigation, Data curation. **Shaoyun Wang:** Methodology, Software. **Chaohui Tong:** Writing - original draft.

Declaration of Competing Interest

The authors declare that they have no known competing financial interests or personal relationships that could have appeared to influence the work reported in this paper.

Acknowledgements

The authors thank the financial supports from the National Natural Science Foundation of China (NSFC project 21774067). C. T. acknowledges the support from K. C. Wong Magna Fund in Ningbo University.

Appendix A. Supplementary data

Supplementary data to this article can be found online at https://doi.org/10.1016/j.chemphys.2020.110810.

References

[1] P.M. Claesson, A. Dedinaite, O.J. Rojas, Adv. Colloid. Interface Sci. 104 (2003) 53–74.
[2] A.V. Dobrynin, Curr. Opin. Colloid Interface Sci. 13 (2008) 376–388.
[3] R. Podgornik, M. Licer, Curr. Opin. Colloid Interface Sci. 11 (2006) 273–279.
[4] H. Boroudjerdi, Y.W. Kim, A. Naji, R.R. Netz, X. Schlagberger, A. Serr, Rhys. Rep. 416 (2005) 129–199.
[5] R.R. Netz, D. Andelman, Phys. Rep. 380 (2003) 1–95.
[6] A. Naji, S. Jungblut, A.G. Moreira, R.R. Netz, Physica A 352 (2005) 131–170.
[7] P.M. Claesson, E. Poptoshev, E. Bloomberg, A. Dedinaite, Adv. Colloid Interface Sci. 114 (2005) 173–187.
[8] R.G. Winkler, A.G. Cherstvy, Adv. Polym. Sci. 255 (2014) 1–56.
[9] R.G. Winkler, A.G. Cherstvy, Phys. Rev. Lett. 96 (2006) 066103.
[10] A.G. Cherstvy, Biopolymers 97 (2012) 311–317.
[11] T. Wallin, P. Linse, J. Phys. Chem. B 101 (1997) 5506–5513.
[12] R.R. Netz, J.F. Joanny, Macromolecules 32 (1999) 9013–9025.
[13] X.K. Man, S. Yang, D.D. Yan, A.C. Shi, Macromolecules 41 (2008) 5451–5455.
[14] X.K. Man, D.D. Yan, Macromolecules 43 (2010) 2582–2588.
[15] J. Wagner, G. Erdemci-Tandogan, R.J. Zandi, Phys.: Cond. Mat. 27 (2015) 495101.
[16] H.M. Li, Y.W. Chen, Y.J. Zhu, C.H. Tong, Chin. J. Polym. Sci. 34 (2016) 552–562.
[17] C.H. Tong, Y.J. Zhu, H.D. Zhang, F. Qiu, P. Tang, Y.L. Yang, J. Phys. Chem. B 115 (2011) 11307–11317.
[18] S.J. De Carvalho, R. Metzler, A.G. Cherstvy, New J. Phys. 18 (2016) 083037.
[19] S.J. De Carvalho, R. Metzler, A.G. Cherstvy, Soft Matter 11 (2015) 4430–4443.
[20] W. Chen, T.J. McCarthy, Macromolecules 30 (1997) 78–86.
[21] A.Y. Grosberg, T.T. Nguyen, B.I. Shklovskii, Rev. Mod. Phys. 74 (2002) 329–345.
[22] J. Faraudo, A. Martin-Molina, Curr. Opin. Colloid Interface Sci. 18 (2013) 517–523.
[23] G.J. Fleer, M.A. Cohen Stuart, J.M.H.M. Scheutjens, T. Cosgrove, B. Vincent, Polymers At Interfaces, Chapman & Hall, London, 1993.
[24] W.L. Chen, R. Cordero, H. Tran, C.K. Ober, Macromolecules 50 (2017) 4089.
[25] M.P. Weir, S.Y. Heriot, S.J. Martin, A.J. Parnell, S.A. Holt, J.R.P. Webster, R.A.L. Jones, Langmuir 27 (2011) 11000.
[26] I. Szleifer, M.A. Carignano, Adv. Chem. Phys. 94 (1996) 165.
[27] S.T. Milner, T.A. Witten, M.E. Cates, Macromolecules 21 (1988) 2610–2619.
[28] A. Halperin, M. Tirrell, T.P. Lodge, Adv. Polym. Sci. 100 (1991) 31–71.
[29] A. Naji, C. Seidel, R.R. Netz, Adv. Polym. Sci. 198 (2006) 149–183.
[30] S. Das, M. Banik, G. Chen, S. Sinha, R. Mukherjee, Soft Matter 11 (2015) 8550–8583.
[31] O.V. Borisov, E.B. Zhulina, T.M. Birshtein, Macromolecules 27 (1994) 4795–4803.
[32] P. Pincus, Macromolecules 24 (1991) 2912.
[33] R. Israels, F.A.M. Leermakers, G.J. Fleer, E.B. Zhulina, Macromolecules 27 (1994) 3249–3261.

[34] C.H. Tong, J. Chem. Phys. 143 (2015) 054903.
[35] C. Kang, S.L. Zhao, C.H. Tong, Chin. J. Polym. Sci. 35 (2017) 98–107.
[36] H. Merlitz, C. Li, C.X. Wu, J.U. Sommer, Soft Matter 11 (2015) 5688–5696.
[37] F. Zhang, S.Y. Wang, H.D. Ding, C.H. Tong, Soft Matter 15 (2019) 2561–2570.
[38] J.F. Kolb, R.P. Joshi, S. Xiao, K.H. Schoenbach, J. Phys. D: Appl. Phys. 41 (2008) 234007.
[39] Z.Y. Tong, Y.J. Zhu, C.H. Tong, Chin. Phys. B 23 (2014) 038202.
[40] T. Kato, M. Kawaguchi, A. Takahashi, T. Onabe, H. Tanaka, Langmuir 15 (1999) 4302.
[41] F.L. Berre, M. Malmsten, E. Blomberg, Langmuir 17 (2001) 699.
[42] Y. Kamiyama, J. Israelachvili, Macromolecules 25 (1992) 5081.
[43] E.B. Zhulina, A.V. Dobrynin, M. Rubinstein, Eur. Phys. J. E: Soft Matter Biol. Phys. 5 (2001) 41.
[44] A.V. Dobrynin, S.P. Obukhow, M. Rubinstein, Macromolecules 32 (1999) 5689.
[45] H. Schiessel, A. Blumen, J. Chem. Phys. 104 (1996) 6036.
[46] D.L.Z. Caetano, S.J. de Carvalho, R. Metzler, A.G. Cherstvy, Phys. Chem. Chem. Phys. 19 (2017) 23397.